Supramolecular self-organization in non-crystalline hybrid organic–inorganic nanomaterials induced by van der Waals interactions

Frédéric Lerouge, Geneviève Cerveau and Robert J. P. Corriu*

Received (in Montpelier, France) 10th March 2006, Accepted 16th May 2006
First published as an Advance Article on the web 14th June 2006
DOI: 10.1039/b603655d

Nanostructured hybrid organic–inorganic solids are a class of materials of growing interest because of their great potential in synthesis and applications. All the molecular organic precursors containing at least two $Si(OR)_3$ groups can be transformed into silica-based hybrid materials by hydrolytic sol–gel polycondensation. These materials exhibit the chemical and physical properties of the organic units included in the silica matrix. They present both nanometric and micrometric scale organization in the solid state, whatever the nature and the geometry of the organic units (linear, twisted, planar and even tetrahedral). These materials are prepared under kinetic control with a corresponding organization that is completely different to crystalline order. Self-organization on a nanometric scale occurs in solution due to the irreversible Si–O–Si bond formation that brings the organic units close to each other, favoring supramolecular van der Waals type interactions by decreasing the entropy. Micrometric scale organization takes place during ageing in the solid state. Densification of the Si–O–Si framework and reorganization of the micrometric aggregates generates stresses that are released by the formation of cracks that lead, upon propagation, to a birefringence phenomenon.

Introduction

The chemistry of organic–inorganic hybrid materials is expanding, thanks to the wide range of possibilities that it opens

Frédéric Lerouge earned a B.S. degree in Chemistry from Bourgogne University (Dijon, 1998) and a M.S. in Molecular Chemistry from the University of Montpellier II (2000). He pursued his PhD with Prof. Corriu and Prof. Cerveau, working on the study of self-assembly processes in nanostructured hybrid materials. He received his PhD in 2003 and is now a postdoctoral fellow in the Institut for Materials Science (ICMAB) in Barcelona.

Geneviève Cerveau is a Professor at the University of Montpellier II (University Institute of Technology). She was first involved in coordination chemistry and stereochemistry at silicon. She then worked in the synthesis of hypervalent species of silicon and germanium, and in the study of their reactivity. Her main scientific interests are now focused on the nanostructured hybrid organic–inorganic materials formed by inorganic polymerisation (sol–gel processes) and especially the study of the factors controlling their organization.

Laboratoire de Chimie Moléculaire et Organisation du solide, UMR 5637, Université Montpellier II, cc 007, Place E. Bataillon, F-34095 Montpellier Cedex 5, France. E-mail: corriu@univ-montp2.fr. E-mail: gcerveau@univ-montp2.fr; Fax: + 33 4 67 14 38 52

Robert Corriu, born in 1934, started his academic career in 1957 as an Assistant at the University of Montpellier. He obtained his PhD in 1961 on the determination of carbocations in strong acids by Raman spectroscopy. In 1964 he became a Professor at the University of Poitiers, and went back to Montpellier as full Professor in 1969. Since 2002 he has been an Emeritus Professor. In 1991 he was elected to a national position at the Institut Universitaire de France as the Chair of Molecular Chemistry. In the same year, he was also elected to the Institut de France (National Sciences Academy) and, in 2001, he became a founder member of the National Academy of Technologies. He has been awarded by the French Chemical Society the SUE Award (1969) and LEBEL Award (1985), JSPS (1981), ACS Kipping (1984), Humboldt Foundation (1992), Max Planck Society (1992), and more recently obtained the Wacker (1998) and Wittig–Grignard (2005) prizes. After a long period of working in organosilicon, organophosphorus and coordination chemistries, his main scientific interests are now focused on the materials formed by inorganic polymerisation (sol–gel type). His knowledge of main group (Si, P) and coordination chemistries is the basis for his work on hybrid materials and mesoporous solids on the way to interactive nanomaterials.

up for expanding access to new kinds of nanomaterials. This field of research bridges different areas of chemistry (organic, inorganic, coordination, *etc*.) and materials science, and also offers many possibilities in terms of physical properties.

Inorganic polymerization represents the most common route to nanomaterials.[1] It corresponds to the formation of oxides by the hydrolytic polycondensation of molecular precursors.[2] Since its discovery by Ebelmann in 1848, it is now known as the sol–gel process.[3] It is worth noting that this purely mineral synthesis is the sister of organic polymerization, since it works in solution at room temperature. The main reaction involved in this process is nucleophilic substitution, induced by the oxygen atom of H_2O, at the metallic center of an alkoxide molecule[4] leading to the formation of Si–O–Si bonds, the propagation of which results in the formation of an oxide.[2] Scheme 1 represents the different stages of the hydrolysis of $Si(OR)_4$ leading to silica.[5]

This is a very convenient way for the preparation of hybrid nanomaterials since, in one step, it is possible to obtain a solid *via* a tuneable colloidal sol (step 3), opening up the possibility of performing coatings, or obtaining a fiber or a matrix.

This methodology represents a very efficient and powerful tool, since it makes materials science compatible with many different aspects of chemistry that were initially separated: solid state, organic, inorganic, organometallic, coordination and macromolecular chemistry, and also biomolecules.[6–13] Thus, a large variety of hybrid materials have been obtained,[14–43] which include organic groups (alkyl, aryl, ...), chelating systems (cyclames, crown ethers, porphyrins) and polymers. All the systems studied up to now are covalently bonded to the inorganic matrix (Scheme 2).

The terminology "chimie douce"[1a] was introduced to emphasize the contrast between the usual high temperature solid-state chemistry, which leads to thermodynamically-controlled materials,[44,45] and sol–gel type processes working under kinetic control at room temperature. Thus, the route illustrated in Scheme 1 can be extended to solids other than SiO_2, opening up a new chemistry that leads to organic–inorganic hybrid materials.

The presence of an R group attached to silicon introduces drastic changes compared to tetraalkoxysilanes. The first change is reactivity, which differs from $Si(OR)_4$. The second is connected with the properties (physical, chemical and also biological) that can be introduced by the molecular units. The third corresponds to the loss of tetrahedral symmetry, thus permitting anisotropic organization in such amorphous solids.

At the present time, two types of self-organization of organic units inside hybrid materials are known. One is induced by van der Waals interactions between organic groups, and the other, totally different, results from H-bonding networks.

A nice example of the latter is the H-bond network issued from the presence of urea groups, which favor the structuring of hybrid solids.[46–52] Here, H-bonds between urea fragments, introduced by the use of proper trialkoxysilanes, are the origin of the organization observed in the resulting solids. Three types of organization were obtained: (a) lamellar-bridged solids in the case of precursors containing aliphatic moieties such as $(CH_2)_{12}$.[46,52] This shows that exploiting the cooperative effects of the molecular interactions, created by long hydrophobic hydrocarbon chains and H-bonding between urea groups in the precursors, favors the nanostructuring of the resulting hybrid solid (Scheme 3a); (b) a crystalline hybrid solid where a rigid phenylene group is directly connected to two urea groups (Scheme 3b)[50,51]; and (c) right- or left-handed helical fibers in the case of hydrolysis–polycondensation of corresponding (*R*,*R*)- and (*S*,*S*)-enantiomers, demonstrating the transcription of chirality from the enantiomers to the hybrid solids (Scheme 3c).[47–49]

Recently, we reported that tetrathiafulvalene derivatives (TTF), substituted *via* a spacer group containing a carbamate function by two or four trialkoxysilyl hydrolysable groups, led

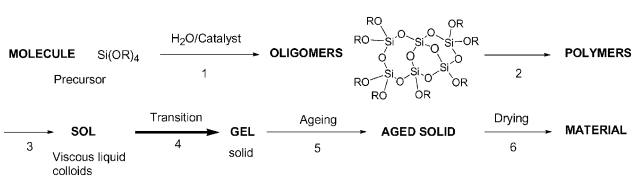

Scheme 1 *Chimie douce*:[1a] Inorganic polymerization of a silica precursor.

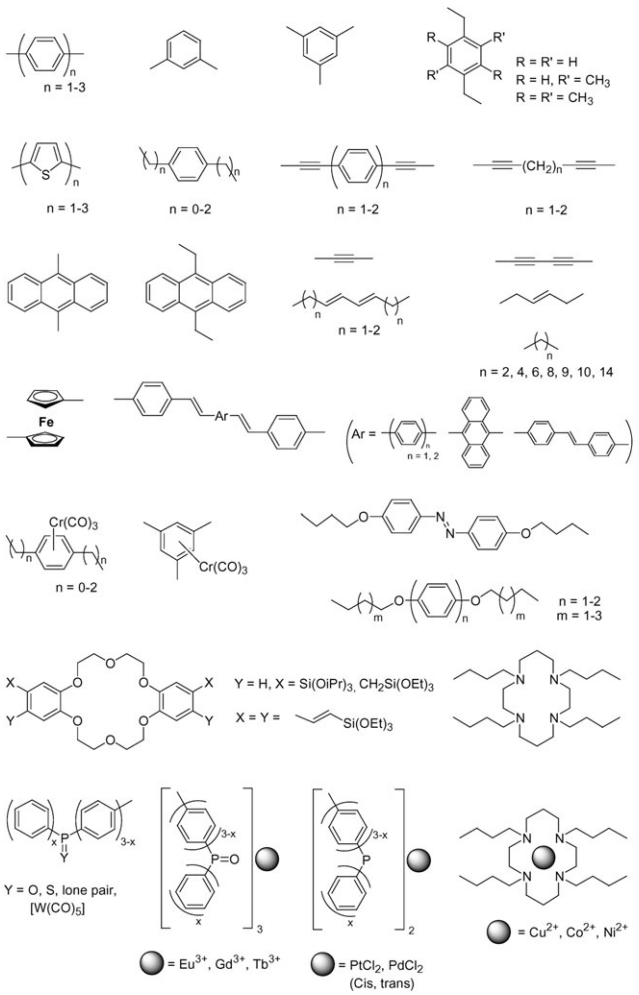

Scheme 2 Examples of organic and organometallic groups introduced into nanostructured hybrid materials.

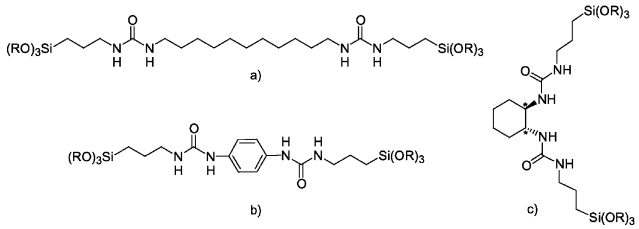

Scheme 3 Precursors presenting H-bonding interactions between urea groups.

to materials organized at both nanometric and micrometric scales.[53,54]

In this case, the carbamate groups play a role in the organization of the materials by H-bonding (Scheme 4).

In the above examples, the energy of the H-bond network, whose directionality dictates the organization of the final material, lies in the range 5 to 10 kcal mol^{-1}.

This paper will focus on the self-organization of molecular units in nanostructured solids which are solely promoted by van der Waals interactions, in the absence of any additive or templating agent.

A description of the sol–gel route: From molecular precursors to silicon-based hybrid organic–inorganic materials

It is important to stress the different stages in the elaboration of a final hybrid organic–inorganic solid. The process starts from a homogeneous solution of the precursor in a solvent, and leads to the formation of soluble species: oligomers, polymers, cross-linked chains and colloids. They result from chemical reactions occurring in solution before the sol–gel transition. Then, once the gel is formed (solid), the syneresis and ageing become important steps, since chemical and physical transformations still occur and strongly influence the characteristics of the material (Scheme 5). Finally, the xerogel is obtained after elimination of the solvent and drying.

Kinetic control is a very powerful tool in designing these solids. All the parameters involved in the kinetics of the hydrolysis–polycondensation reaction (temperature,[55] concentration of reagents, concentration and nature of the catalyst,[56] solvent,[56a] leaving group, methodologies, *etc.*) can be used to change and optimize the solid's texture (specific surface area, porosity). For a given precursor, changes to the solvent or the catalyst modify drastically the texture of the resulting materials.[57] The texture can be considered a result of a very complex process, in which all the experimental parameters play a role.[57] Table 1 and Table 2 provide some examples concerning the solvent effect[56a] and the influence of ageing temperature[55d] on the textural properties.

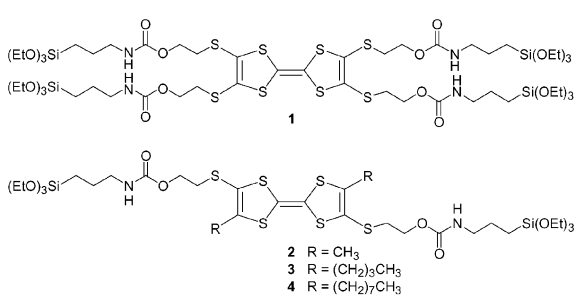

Scheme 4 TTF groups introduced in nanostructured hybrid materials.

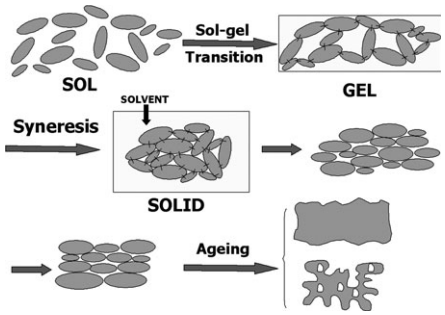

Scheme 5 Schematic representation of the sol–gel process.

The effect of ageing temperature is very illustrative, since at low temperatures (−20 °C), resin-type materials are obtained (low specific surface area and no porosity), while at higher temperatures (+55 °C), a narrow pore size distribution is observed. These observations illustrate the dramatic importance of ageing. It is worth mentioning that, until this work, the effect of temperature on polycondensation or ageing had never been considered.

What kind of organization is there for silicon-based hybrid organic–inorganic materials?

In the case of these hybrid solids, the situation is different to silica made of SiO_4 tetrahedrons of high symmetry. Indeed, the presence of an R group decreases the symmetry of SiO_2 and allows interactions between the organic units, which can drastically influence the final structure and organization of the solid.

In this paper, we will only consider nanostructured materials obtained from precursors containing at least two Si–C bonds. However, we will briefly mention below two examples concerning polysilsesquioxanes of general formula R–$SiO_{1.5}$ exhibiting layered structures.[58–68] In the case of R = octadecyl, hydrolysis leads to the formation of a solid with a highly organized lamellar structure, consisting of periodically alternating alkyl chains layers and siloxy backbones (Scheme 6).[58–63] The alkyl chains can also be covalently bonded to an inorganic layer made of an Si–O–M network (M = Mg,[64–67] Al,[64–66] Cu,[67] or Ni[68]), as illustrated in Scheme 6.

The second example concerns the hydrolytic polycondensation of a supramolecular network of bis-silylated carbamate salts, leading to well-defined lamellar structures (Scheme 7).[69] The loss of CO_2, achieved upon heating, generates materials that contain free amino groups, in which the lamellar structure is maintained.

Due to their starting shape, a different situation is observed in the case of materials obtained from precursors bearing two $Si(OR)_3$ groups. Taking into account the experimental data corresponding to hybrid materials (spectroscopic and textural), different types of organizations of the organic units can be envisaged, as shown in Scheme 8. **A** corresponds to complete

Table 1 Solvent effect on the textural properties of hybrid solids

Precursor	X	Concentration/mol l^{-1}	Solvent	Catalyst (mol %)	Temperature/°C	Specific surface area/m^2 g^{-1}
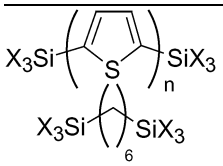	OMe	1	MeOH	NH_4F (1)	20	685
	OMe	1	THF	NH_4F (1)	20	20
	OEt	0.4	EtOH	HCl (10.8)	20	<10
	OEt	0.4	THF	HCl (10.8)	20	380

Table 2 Temperature effect on the textural properties of hybrid solids[a]

Precursor	Solvent	Temperature (°C)		BET measurements		
		Gel	Ageing	SSA/m^2 g^{-1}	μ-pores (%)	Pore size/Å
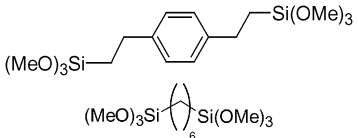	THF	−20	−20	<10	—	—
	THF	−20	+55	715	5	40
	THF	−20	−20	<10	—	—
	THF	−20	+55	865	0	80

[a] SSA = specific surface area.

disorder, leading to a random structure; **B** and **C** represent different structures, in which the organic units are not randomly organized.

Chemical behavior and self-organization

Initially, chemical reactivity of some of the nanostructured solids (possibility to achieve polymerization in the solid state between the organic groups) suggested the idea of a short range order organization existing in these materials.[11] This was performed in the case of xerogels containing mono and terthiophene units. In these materials, an electrochemically induced polymerization of thiophene units was obtained, leading to a silica–polythiophene composite.[70] In the case of xerogels containing butadiyne moieties, polymerization occurs at 200 °C, leading to a polydiyine–silica composite.[71] In both examples, the organic groups have to be close enough to react with each other and the coupling reactions involve very severe stereochemical requirements. In the case of thiophene, the coupling of two radical cation species implies parallelism between thiophene units,[70] which can also be seen with butadyine units (Scheme 9).[71]

Another example is the specific properties of chelating units of solids prepared from tetraazamacrocycles (cyclame precursors).[72,73] The cyclame, bearing four $(CH_2)_3Si(OEt)_3$ groups on the nitrogen atoms, permits nanostructured materials to be obtained, in which a self-organization has been evidenced by

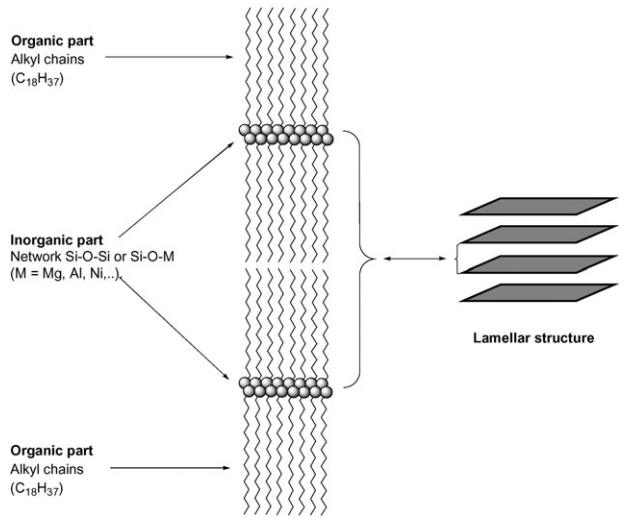

Scheme 6 Schematic representation of a layered structure for polysilsesquioxanes.

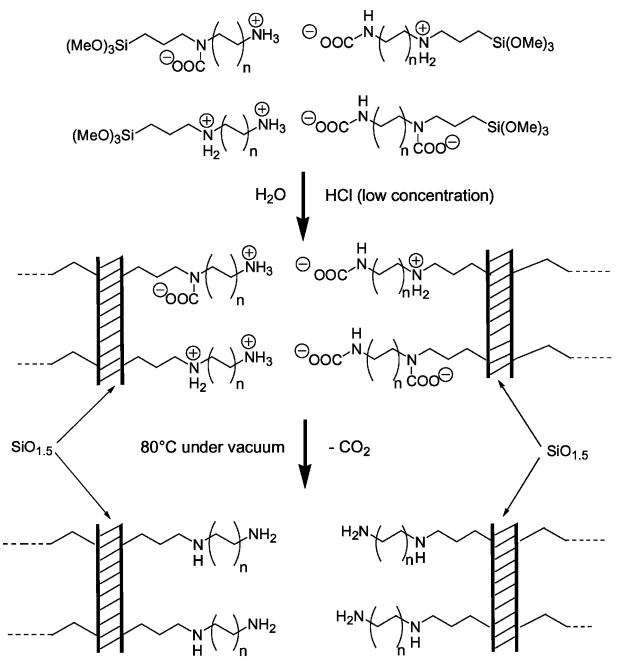

Scheme 7 Lamellar structure of amine-functionalized silica where n = 1 or 3.

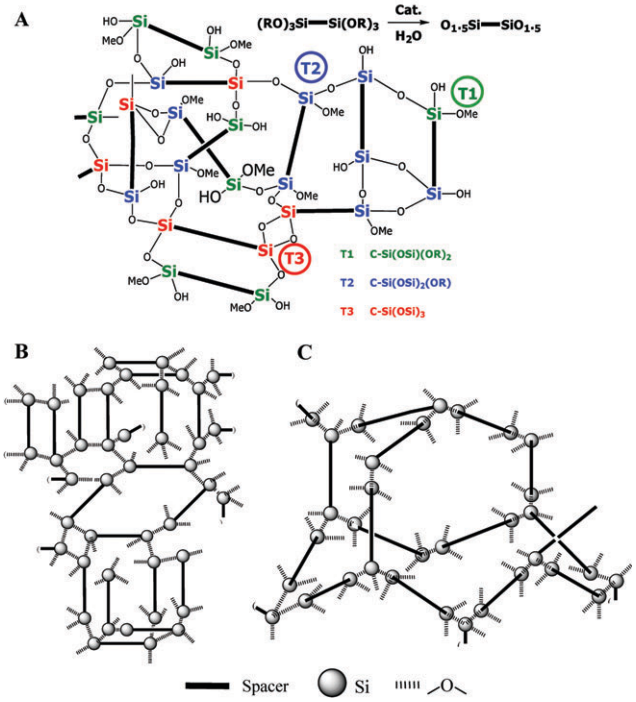

Scheme 8 Schematic representation of three different types of auto-organization of organic units.

the ability of the chelating units to complex lanthanides (Eu^{3+}, Er^{3+}, Gd^{3+}), corresponding to the incorporation of 1 lanthanide per 2 cyclame units (Scheme 10).[72] Such behavior is unexpected since, in solution, without substitution by amido groups at nitrogen, tetraazamacrocycles are not chelating units for lanthanides.

A comparison between two routes for the incorporation of copper salts within cyclame-containing hybrid materials is of great interest (Scheme 11).[73a] The incorporation of Cu^{II} centers into materials by route B gives rise to Cu–Cu interactions that are not observed when the metal centers are introduced by route A, as shown by X-band ESR spectroscopy (Scheme 11). Such a phenomenon has been observed in solution in the case of dinuclear Cu^{II} complexes, in which two cyclame rings are in a face-to-face geometry (C, Scheme 11). These differences arise because of the difference between the two solids obtained from two different precursors. In route A, the precursor is a cyclame complexed with Cu^{2+} and 2 Cl^{-}, completely different to the precursor used in route B, which is a flexible cyclame derivative without any ionic charge. The materials obtained by the two routes exhibit very different organizations of the organic units; route B permitting the organization of cyclame units.

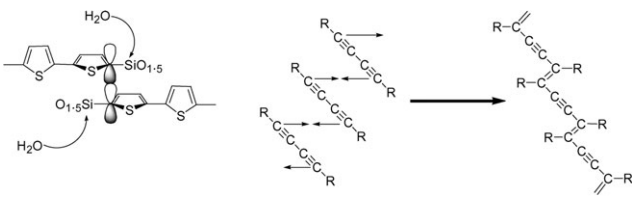

Scheme 9 Stereoelectronic requirements for the coupling of thiophene or butadiyne units.

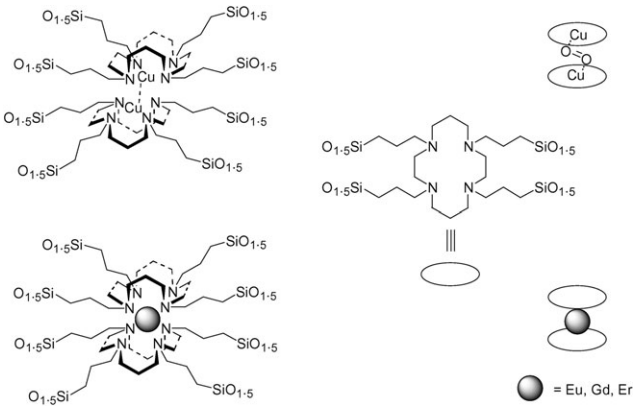

Scheme 10 Representation of cyclame complexes.

These results are in good agreement with the complexation of Cu atoms that are able to fix dioxygen in the ratio 1 O_2 to 2 Cu; the oxygen molecule being reversibly chelated between the 2 Cu atoms (Scheme 10). Both results, demonstrated by EXAFS, can only be explained by an initial organization of the cyclame units in the solid.[73] All of these chemical transformations are indicative of a short-range order in the solid state, since they require the proximity of the organic groups for chelating lanthanide ions or are required to organize the cooperation between the two Cu^{2+} ions. Coordination chemistry in the solid state is not a copy of that in solution because it depends on the solid state organization. In the solid state, the chelating units are static. In contrast, they can exhibit an organization.

Study of the self-organization

The phenomenon of self-organization during the hydrolytic polycondensation arises only from hydrophobic interactions between the organic groups. This reaction has always been performed in solution with a stoichiometric amount of water; other parameters being adjustable. As for the texture, it appears that self-organization is kinetically controlled and depends on the experimental parameters (temperature, nature and concentration of the reagents, catalyst, solvent, *etc.*).

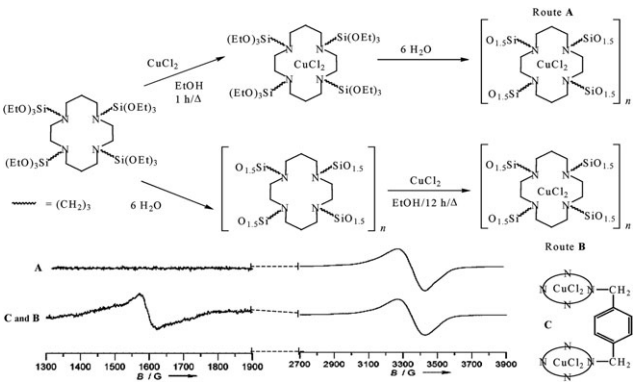

Scheme 11 Different types of organization observed, depending on the method of preparation. Route A: complexed cyclame. Route B: free cyclame. X-band ESR spectra recorded at 100 K of the allowed transitions for materials of routes A and B, and for molecular complex C.

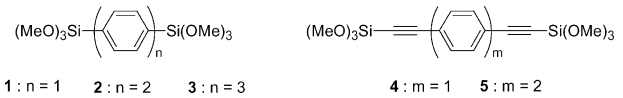

1 : n = 1 2 : n = 2 3 : n = 3 4 : m = 1 5 : m = 2

Scheme 12 Linear precursors **1–5**.

The study of this phenomenon was based on two types of technique. Firstly, a X-ray diffraction study allowed the detection of organization at a nanometric scale. At the micrometric (and sometimes millimetric) scale, the organization of hybrid materials is revealed by their birefringence under cross-polarized light. In addition, the optical axis gives information about the orientation of this organization.

The case of linear systems

Linear rigid molecular precursors of different sizes were first investigated.[74] The precursors, **1–5**, were synthesized and polycondensed under the same experimental conditions (Scheme 12).

Looking at the X-ray diffraction (XRD) patterns of the xerogels (Fig. 1), the absence of any sharp Bragg signals is evidence of the absence of crystal organization.

However, the presence of broad signals indicates an organization on the nanometric scale. It is clear that these signals are the result of an organization between the organic units, since they are always additional to the signal at 3.5 to 3.7 Å, attributed to the Si–O–Si contribution. However, it is important to underline that, despite the fact that these peaks are too large to be interpreted in terms of crystalline periodicity over a long range, a short-range order in the hybrid solid can be considered, and is possibly favored by rigid organic units. Assuming *a priori* Bragg's law, the distance associated with the peak at the lowest q value corresponds to the Si···Si distance in the organic spacer, as determined by molecular simulation (Table 3).[74]

The densification of the solid occurs when the molecules of water disappear progressively, while molecules of alcohol appear. Thus, the organic units are under conditions that favor self-organization. Indeed the formation of Si–O–Si bonds transforms the *intermolecular* interactions into *intramolecular* interactions, favoring a decrease in entropy (Scheme 13). This decrease in entropy allows the existence of organization between the organic spacers thanks to lipophilic van der Waals interactions, of which the energy, inversely proportional to the distance (r^{-6} law), is too low to allow similar organization in solution.

Physical evidence of micrometric scale organization in the solid state was obtained by birefringence experiments.[74] This

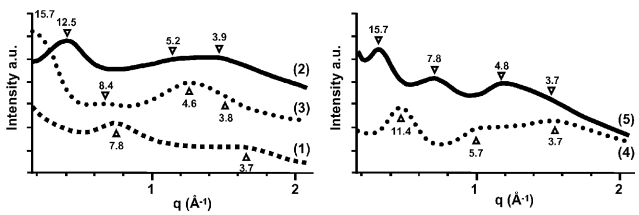

Fig. 1 X-Ray diffraction patterns of nanostructured materials obtained from **1–5**.

Table 3 Comparison between the experimental and calculated values for Si···Si distances

	Distances/Å		
	Precursor	Calculated	Experimental
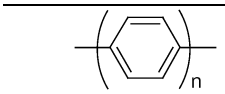	**1** (n = 1)	7.8	7.8
	2 (n = 2)	12.3	12.5
	3 (n = 3)	15.7	16.3
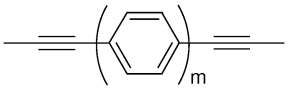	**4** (m = 1)	11.5	11.4
	5 (m = 2)	15.5	15.7

scale corresponds to the wavelength range of the white light used for measurements. The sol was introduced into a Teflon-coated cell just before the sol–gel transition. After a few minutes, bright domains appeared in various spots. A few hours later, the whole cell was birefringent and some cracks had appeared (Fig. 2).

The formation of cracks was observed in almost all cases due to shrinkage following the polycondensation at silicon. The formation of Si–O–Si bonds changes the precursor molecules (monomers), which are isolated in solution, into a denser medium, finally giving a solid in which all the silicon atoms are linked to one other. Thus, black isotropic regions corresponding to void are observed between the birefringent chunks of gel.

Dynamic studies have been performed in order to determine during which step of the sol–gel process birefringence occurs.[74a] Experiments were realised with a controlled partial pressure of water, using open cells containing the pure crystalline precursor **4** (Scheme 12), which can be polycondensed without catalyst. Fig. 3 shows the slow apparition of birefringence after the sol–gel transition.

This experimental procedure allows the history of xerogel formation to be traced through the successive states: precursor, oligomers, polymers, sol, gel and cracks. It permits the conclusion that extension of the organization at a micrometric scale occurs during the ageing of the solid. A schematic representation of this experiment is given in Scheme 14.[74a]

Initially, the highly birefringent solid **4** (H) occupies the whole cell (step 1). After a few minutes, the solid (H) at the edge of the cell is converted into an isotropic liquid (I) (step 2). In step 3, (I) is formed deeper in the cell, and at the same time a new birefringent solid (J) appears. Then, cracks (K) are formed due to the syneresis and ageing (step 4).

A study on the origin of birefringence in a hybrid gel containing a phenyl group, formed by polycondensation, shows that it appears during gel shrinkage.[75] The gel organization can be related to a tensile strain due to inhomogeneous

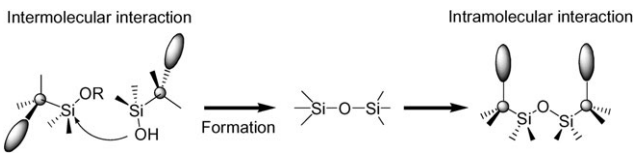

Scheme 13 A decrease in entropy induced by Si–O–Si bond formation.

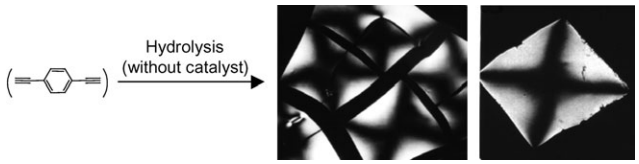

Fig. 2 Birefringence pictures of a xerogel obtained from **4** (Scheme 12).

solvent evaporation. The birefringence is induced by a strain field anisotropy during gel ageing, as revealed by simultaneous dynamic light scattering and birefringence measurements.[75]

These studies show that hydrolytic polycondensation leads to two types of organization: a nanometric scale organization, which appears during polycondensation, and a micrometric one, which takes place during the rearrangements that occur during the ageing of the solid. It is important to underline the fact that the two stages of organization take place during two different phases. The first one occurs in solution, and goes on until the formation of micrometric-sized colloids, leading to an isotropic sol. The second one corresponds to reorganizations in the solid state during ageing, and depends on the nature of the organic spacer and on the formation of cracks. The nanometric and the micrometric organizations are independent of each other. However, they are both under kinetic control.

Generalization of the self-organization phenomenon

It has been clearly demonstrated that the phenomenon of self-organization is a general one. Scheme 15 shows some of the systems presenting different geometries that have been studied.[76]

The following similar characteristics have been found in all cases: (1) an X-ray diffraction pattern exhibiting signals characteristic of the molecular spacer and indicative of a nanometric scale organization; (2) emergence of birefringence during the ageing of the solid; (3) formation of cracks corresponding to the transition from a colloidal solution of cross-linked polymers to a polycondensed solid; (4) the presence of a wide variety of birefringence pictures, strongly depending on the nature of the precursor; (5) orientation of the optical axis, strongly dependent on the geometry of the precursor. Points 2–5 correspond to different organizations at a micrometric scale. A schematic representation of the organization is given in Scheme 16.

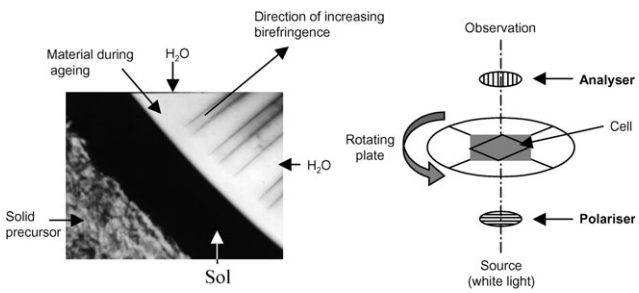

Fig. 3 Dynamic representation of birefringence formation and a schematic of birefringence measurement.

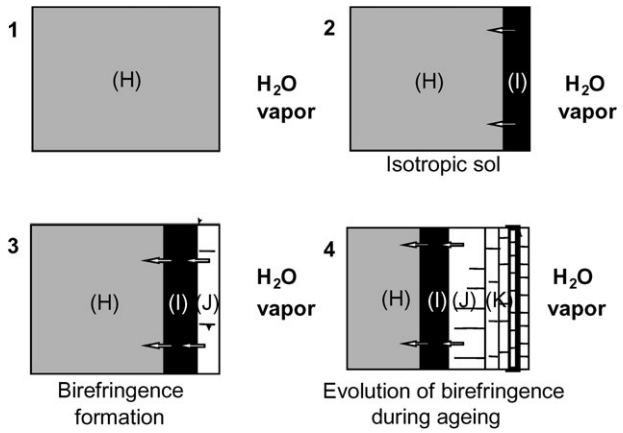

Scheme 14 Birefringence experiments: Evolution of part of a cell during the polycondensation process: (1) precursor, (2) sol formation, (3) birefringence and (4) evolution of birefringence during ageing.

The case of aliphatic precursors $(RO)_3Si(CH_2)_nSi(OR)_3$ is particularly interesting. Although the hybrid solids exhibit X-ray diffraction patterns, no birefringence is observed.[74b] Such a result can be explained by the hydrophobic behavior of aliphatic systems placed under the hydrophilic conditions required for hydrolytic polycondensation. During the process, hydrophobic $Si(OR)_3$ groups are modified into hydrophilic $Si(OR)_2(OH)$. Thus, the hydrophobic flexible aliphatic chains amalgamate into a spheroidal micelle-type geometry (Scheme 17). Finally, the stacking of these species during ageing leads to isotropic materials.

The case of tetrahedral precursors

Precursors presenting a rigid tetrahedral geometry have been studied in order to determine the limits of self-organization.[77] This geometry is known to favor isotropy, and no liquid crystals properties have been reported. For instance, molecules having a tetrahedral core and bearing eight long aliphatic groups $[O(CH_2)_9CH_3]$, explored as possible mesophases (Scheme 18), do not present any birefringence properties,[78] proving that the lipophilic interactions between the eight chains are not enough to induce an intermolecular self-organization.

It is interesting to note that linear systems presenting two short chains can exhibit birefringence properties (Scheme 19).[79]

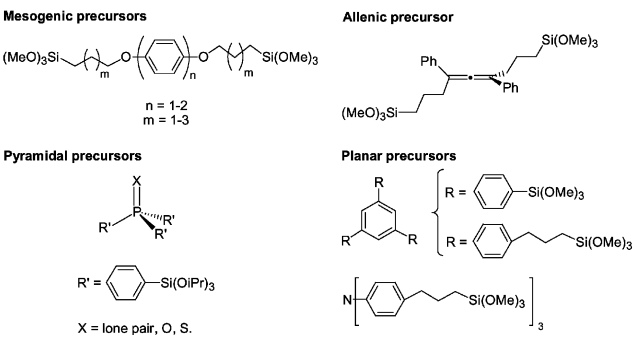

Scheme 15 Molecular precursors leading to materials organized at nanometric and micrometric scales.

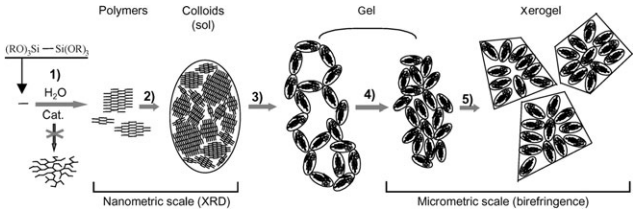

Scheme 16 Control of the auto-organization of nanostructured hybrid materials: A schematic representation of the different steps involved in the process.

The linear aromatic core does not present any birefringence properties, however, the presence of aliphatic chains is sufficient to induce smectic or nematic liquid crystal-type anisotropic organization. This comparison clearly demonstrates that a tetrahedral geometry does not favor anisotropy.

Studies have been performed on the cases of precursors presenting tetrahedral carbon, germanium and tin central atoms with twelve directions for solid formation, oriented regularly at the four directions of the tetrahedron (Scheme 20).[77]

The hydrolytic polycondensation of these precursors that do not bear any mesogenic groups induces an organization on a nanometric scale and another on a micrometric one. As for all other nanostructured hybrid materials, the X-ray diffraction patterns exhibit broad and intense signals that correspond, without any doubt, to the existence of a nanometric order in the materials. For example, in the case of the tin compound, the strongest signal at $\sim$7 Å can be correlated with values obtained by molecular modelling, and corresponds to the distance separating the mean planes constituted of tin atoms on the one hand and siloxane bridges on the other. The birefringence pictures correspond to an anisotropic medium organized at a micrometric scale (Fig. 4).[77]

The size and arrangement of the rod-like chunks is regular. The optical axes are oriented perpendicularly to the edges of the chunks (Fig. 4). This corresponds to an orientation of the organized matter at a micrometric scale, when in the case of liquid crystals, it is connected with the orientation of independent molecules, anisotropically organized. These results, observed in the case of tetrahedral units, clearly show that the self-organization process is a general one, since it occurs even when the organic precursor presents a geometry that favors isotropy. Furthermore, the regularity of the size and distribution extends from a micrometric to a centimetric scale.

This example demonstrates clearly that a high level of organization can be reached by hydrolytic polycondensation. The formation of Si–O–Si bonds drastically minimizes entropy (Scheme 12) and thus allows the self-organization of non-

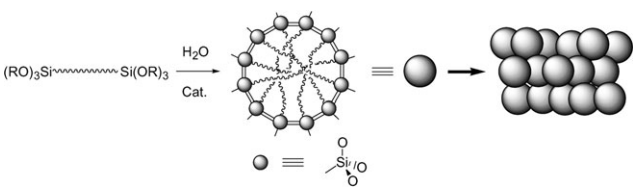

Scheme 17 Globular-type aggregates obtained from aliphatic systems.

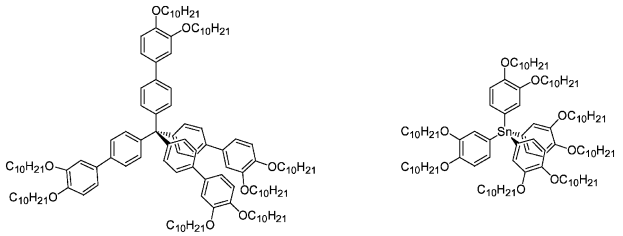

Scheme 18 Tetrahedral molecules without liquid crystal properties.

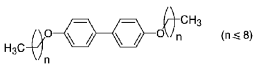

Scheme 19 Linear molecular precursors having liquid crystal behavior.

mesogenic units at three levels: nanometric, micrometric and millimetric.

Kinetic control of self-organization

As mentioned before, the self-organization phenomenon is a kinetically controlled process. Experimental conditions (solvent, catalyst, concentrations of reagents, temperature, *etc.*) have a direct influence on the observed birefringence (form and size of chunks, birefringence intensity, orientation of optical axis), as illustrated in the following examples.

In the case of the allenic precursor, presenting a twisted geometry (Scheme 14), the influence of temperature at the three levels of organization is clearly evidenced, since the X-ray diffraction patterns and the birefringence pictures vary drastically, as seen in Fig. 5 and Fig. 6.[76b] The X-ray pattern exhibits, as usual, two broad signals at room temperature (20 °C). At low temperature (3 °C), additional weak signals, indicative of a better micrometric scale organization, are observed.[76b]

At 20 °C, the birefringence figures show the presence of parallel wavy cracks that propagate throughout the whole cell (2 × 2 cm) over distances of several millimeters. Such a phenomenon has never been observed before. The optical axis is oriented parallel to the edges of the cracks (Fig. 6a). In contrast, at 3 °C, the birefringence appears without cracks and the optical axis is oriented radially about a central point (Fig. 6b).[76b]

The case of tetrahedral precursors is also illustrative, since birefringence is different when using TBAF or HCl as the catalyst (Fig. 7).[77] However, the main characteristics are the same: birefringence intensities, direction of optical axis and extension of organization on a millimetric scale. In both cases, the X-ray patterns are similar.

The same observation has been reported in the case of a planar precursor: birefringence pictures are very different

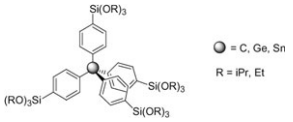

Scheme 20 Tetrahedral precursors.

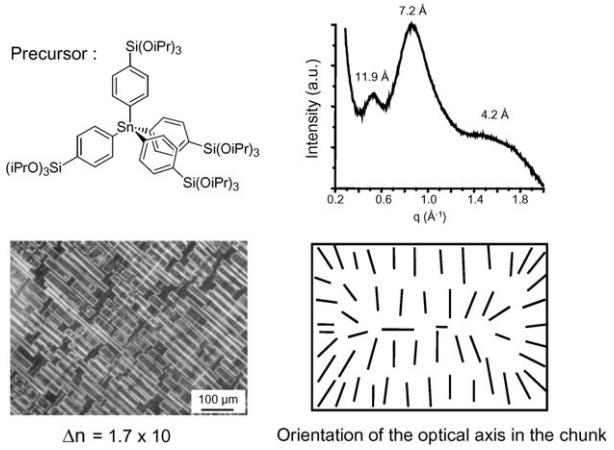

Fig. 4 X-ray diagram and birefringence picture obtained from a tetrahedral precursor.

depending on the catalyst, concentration or temperature (Fig. 8).[76c]

Thus, both the texture and self-organization are under kinetic control. This is of great importance, since it means that it is possible to optimize the physical characteristics of the material by varying the kinetic parameters: solvent, hydrophilic/lipophilic balance, temperature, and the nature and concentration of the reagents and catalyst. The inorganic polymerization allows the texture and organization to be adjusted, the stabilization of the final material being performed by a hydrothermal treatment under rather mild conditions ($T < 150$ °C, acid catalyst in low concentration). Such treatment stops further evolution of the solid by preventing polycondensation at silicon as well as the redistribution of Si–O–Si bonds.

The same parameters control the solid's texture and structure in different ways. Control of the texture corresponds to the organization of the surface of the solid (specific surface area and porosity), while structural control concerns the arrangement of the organic units inside the material.

The self-organization process of organic–inorganic hybrid materials

In the process that goes from a homogeneous solution to a solid, the turning point appears to be the sol–gel transition

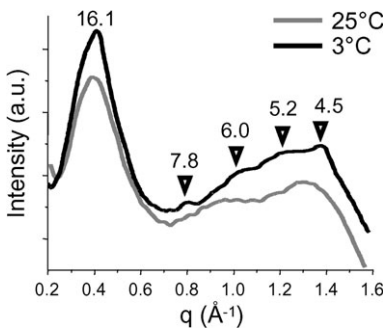

Fig. 5 Influence of temperature on nanometric scale organization.

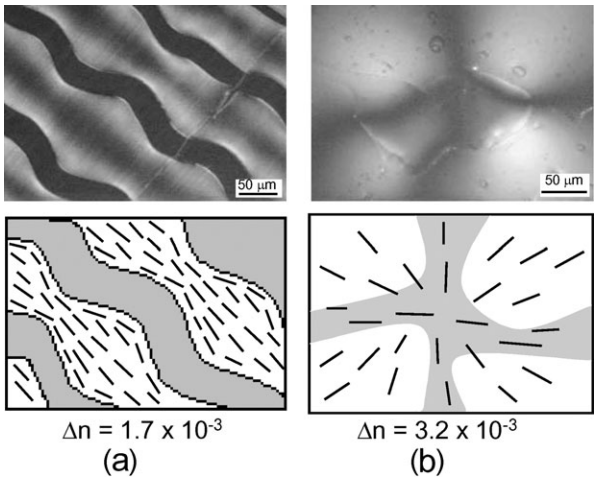

Fig. 6 Influence of temperature on micrometric scale organization: (a) 20 °C and (b) 3 °C.

(Scheme 16, step 3), and the different steps occurring before and after this point must be considered.

The first phase of the organization occurs in solution during the mainly irreversible Si–O–Si bond formation (Scheme 16, steps 1 and 2). Oligomers form and grow, giving polymers by polycondensation. Organic units are brought close to each other and supramolecular van der Waals-type interactions are favored, leading to nanometric scale self-organization. During these steps, the nanometric organization between the organic spacers is built up by the formation of aggregates of different sizes. For this reason, the X-ray diffraction patterns exhibit broad signals instead of Bragg peaks. These aggregates, which are formed of the same elemental "bricks", link covalently to form micrometric-size colloids, constituting the sol, a viscous liquid. Thus, in solution, during the first steps of the polycondensation, the van der Waals interactions between the organic units induce a short range order over nanometric domains.

The formation of covalent bonds between colloids corresponds to the sol–gel transition (step 3, Scheme 16).

The second important phase of the process concerns the changes that occur in the solid state during ageing (Scheme 16, steps 4 and 5). The texture and organization of the solid depend highly on the parameters that control the ageing of the material in the solid state. The birefringence phenomenon and the orientation of the optical axis are the result of the transformations that take place in the solid state. The densification of the Si–O–Si framework, the syneresis step

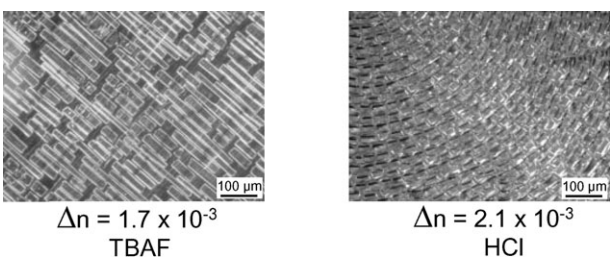

Fig. 7 Influence of catalyst on birefringence properties in the case of a tetrahedral tin precursor.

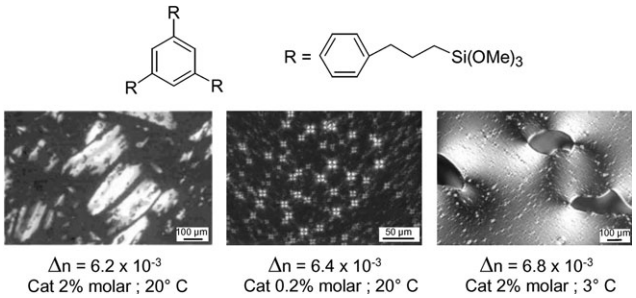

Fig. 8 Influence of concentration of catalyst (TBAF) and temperature on birefringence pictures in the case of a planar precursor.

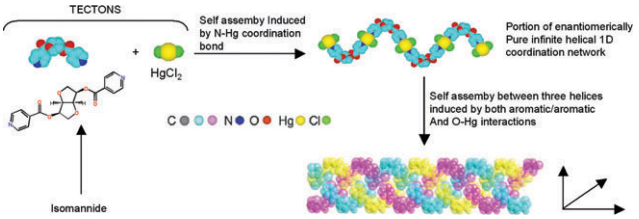

Fig. 9 Formation of an enantiomerically pure, triple-stranded helical coordination network.

(expulsion of the solvent) and the reorganization of the micrometric aggregates generate stresses that are released by the formation of cracks or regions corresponding to the shrinkage of the material. These lead to the birefringence phenomenon due to the propagation of short range order to domains larger than the wavelength of light. The orientation of the optical axis corresponds to an orientation of the organized matter on a micrometric scale.

Nanostructured hybrid solids and crystals

The hydrolytic polycondensation of nanostructured hybrid solids does not correspond to badly-organized crystalline systems or to short range crystalline organization. The way that nanostructured solids are structured is *totally different* to that for crystals, in which the crystal lattice is identical in the three directions of space, as their structure can be different from one direction to another in the case of lamellar or helicoidal systems (Fig. 9). In these cases, as well as in the case of classical crystals, the organization of the elemental lattice is the same in each direction of space. Moreover, crystal growth is under thermodynamic control.

For example, a cubic crystal of NaCl has a lattice that reproduces identically in three dimensions, as for tetragonal or monoclinic crystals. In the case of lamellar crystals such as mica or clays, the crystal has two identical directions corresponding to the plane of the lamellae. The third direction, perpendicular to the two others, corresponds to the stacking of identical lamellae.

The case of unidirectional crystals is less common than the two previous examples. It will be illustrated here by the case of a three-fold helix obtained by an organometallic synthesis (Fig. 9).[80]

Using an enantiomerically pure organic tecton derived from isomannide, the formation of an enantiomerically pure helical coordination network was achieved and structurally characterized by X-ray diffraction on a single crystal. Three infinite helical strands self-assemble into a triple-stranded non-cylindrical architecture through aromatic–aromatic interactions. The triple-stranded helices are packed parallel to each other and further interconnected through O–Hg interactions. The overall structure may be described as a 3-D network resulting from the interconnection of triple-stranded helical 1-D networks. Such organization results from favorable van der Waals interactions.

The type of organization observed in nanostructured hybrid materials that are *stricto sensu* amorphous systems results from a process totally different to crystalline growth. In the case of crystal formation, there is an equilibrium between the solid growth and the solution allowing the crystal growth, only by assembling elemental bricks. In contrast, in the case of self-organization observed during the polycondensation, two different phases have been evidenced, depending on the progress of the process:

(1) Nanometric scale organization (X-ray diffraction), which takes place in solution during the formation of polymers.

(2) Micrometric scale organization (birefringence), which occurs in the solid state during ageing. Moreover, an organization on a centimetric scale between the cracks and the sub-millimetric-sized chunks has been observed in some cases.

Differently to crystals, this organization is not reproduced identically in three dimensions. Indeed, the three levels of organization that are observed correspond to different chemical steps, and they occur during a complex process that presents several phases of evolution. Nanometric organization takes place in solution, whereas its extension to the micrometric then centimetric scales occur in the solid state during ageing. Finally, this whole process is under kinetic control, whereas crystal formation is thermodynamically controlled.

Conclusions

The materials obtained during hydrolytic polycondensation exhibit an organization that appears to be completely different to crystal growth. However, it can extend on a wide scale. The growth of these materials is particular, since different scales of organization can be observed, corresponding to different phases of the process, governed by the different parameters that control the kinetics of polycondensation. In solution, the formation of Si–O–Si bonds forces the molecules closer to each other. This minimizes the entropy, favoring intramolecular van der Waals interactions that can only occur when the organic groups are close enough, since their energy is inversely proportional to the distance according to the r^{-6} law. Thus, self-organization is not spontaneous and corresponds to a close contact that is imposed to precursor molecules during the polycondensation. This hypothesis permits the explanation of the nanometric scale order. After the sol–gel transition, the system is governed by interactions between micrometric-sized particles that become connected. Evolution in the solid state controls the formation of both texture and structure. This

phenomenon is completely different, and is controlled by surface functionalities and the propagation of cracks. This evolution in the solid permits the organization on a micrometric scale (birefringence), which can be, in some cases, extended to a millimetric scale.

Perspectives

Although the chemistry of nanostructured hybrid materials has developed only recently, it opens up wide and interesting perspectives. Firstly, these materials allow the inclusion and organization of a wide number of chemical units inside silica matrices with almost no limitation. It is possible to include entities such as molecules, fragments of polymers, cluster oxides, sulfides or phosphides, *etc*. The only difficulty lies in the synthesis of precursors, since the nanotools that bring the properties must bear at least two hydrolysable $Si(OR)_3$ functional groups, allowing the irreversible formation of silica-like matrices.

The opening towards biomolecules is certainly a very promising field; however, materials incorporating biomolecules have not been studied yet. Nowadays, the most attractive hybrid solids are those obtained from organic or organometallic units that could exhibit useful physical properties. The materials obtained in this way correspond to a new approach to nanomaterials. Thus, it is possible to include entities presenting physical properties inside a silica matrix (Scheme 2). Until now, the properties of these materials had not been especially studied; however, they have interesting potential. In fact, there is no limitation, since entities such as phosphines, tetraazamacrocycles and other chelating units, complexed or not by a metallic ion, have been introduced into SiO_2 matrices (Scheme 2, Scheme 10 and Scheme 11). Coordination in the solid represents a new field of experimentation; the material can be used as a chelating system, opening the way to a coordination chemistry that will be totally different to the one observed in solution. In the solid, the different entities are linked to one another and are located in a defined environment that minimizes entropy. Furthermore, the solid presents possibilities of a fixed organization that does not exist in solution, and which is susceptible to modification by the geometry and level of coordination of metallic ions. Thus, it appears possible to develop a chemistry based on the properties of materials obtained from these solids by the complexation of transition metals and lanthanides. Many of these materials exhibit photoluminescence and/or magnetic properties that could be exploited. Currently, matrices incorporating transition metals and lanthanides have not been particularly developed. However, such matrices would present interesting perspectives, since the existence of chelating units within the matrix might allow metallic nanoparticles to be incorporated. For instance, nanomaterials presenting useful physical properties, such as magnetic (obtained by the incorporation of Fe_3O_4, Fe_2O_3 or NiO nanoparticles) or electric (by incorporation of In_2O_3) ones, might emerge from this type of work. Thus, the possible expansion of new types of nanomaterials, which are likely to present useful optical, magnetic or electric properties and are capable of incorporating supramolecular units, is taking shape.

One of the other prospects in this field consists of the use of non-siliceous matrices. Among numerous examples, SnO_2-based materials could find applications due to its semiconductor properties. TiO_2 is also attractive because of its photovoltaic properties. Iron oxides (Fe_3O_4 or Fe_2O_3) and NiO could lead to magnetic materials, while In_2O_3 exhibits potentially useful electrical properties. This would permit the inclusion of organic units or coordinated metallic ions with exploitable properties inside a matrix which affords its own characteristics. A very attractive topic is the possible access to interactive nanomaterials. However, this goal will require greater developments in the sol–gel chemistry of these oxides, which has not been extensively considered until now. In addition, it will also be important to develop studies concerning ways of allowing the inclusion of organic units. While Ti–C, Fe–C and Ni–C bonds are not stable, the sol–gel approach offers an alternative to this chemistry by using $-Si(OR)_3$ or $-PO(OR)_2$ groups to link organic units to the non-silica oxide matrix.

Finally, the hybrid organic–inorganic materials described here can be used as matrices for the preparation of nanocomposites. So in this way, polytrialkoxysilylated molecular units presenting some exploitable physical properties could be used to build up matrices containing different nanotools, in order to design interactive nanomaterials. The hybrid materials that are described here can play the role of matrix and incorporate organic or organometallic entities with useful physical properties. For instance, one can imagine a magnetic material obtained by the incorporation of lanthanide ion complexes in a matrix that includes molecular units with photoluminescence properties. One may foresee the interesting physical properties that could come out of these types of interactive nanomaterials.

These few examples give a survey of the wide possibilities opened-up by the nanostructuring of hybrid materials.

References

1 (*a*) J. Livage, *Chem. Scr*., 1988, **28**, 9–13; (*b*) C. Sanchez and J. Livage, *New J. Chem*., 1990, **14**(6–7), 513–521; (*c*) J. Livage, *Mater. Sci. Forum*, 1994, **152–153**, 43–54; (*d*) J. Livage, *Bull. Mater. Sci*., 1999, **22**(3), 201–205; (*e*) A. Vioux, *Chem. Mater*., 1997, 2292.
2 *De la solution à l'oxyde*, ed. J. P. Jolivet, InterÉditions, Paris, 1994.
3 (*a*) M. Ebelmann, *Ann. Chim. Phys*., 1846, **16**, 129; (*b*) C. R. Ebelmann, *Acad. Sci*., 1847, **25**, 854.
4 L. L. Hench and J. K. West, *Chem. Rev*., 1990, **90**, 33.
5 C. J. Brinker and G. W. Scherer, *Sol–Gel Science: The Physics and Chemistry of Sol–Gel Processing*, Academic Press, San Diego, 1990.
6 D. A. Loy and K. J. Shea, *Chem. Rev*., 1995, **95**, 1431.
7 *New J. Chem*., special issue, ed. C. Sanchez and F. Ribot, 1994, **18**, 1007.
8 P. Judenstein and C. Sanchez, *J. Mater. Chem*., 1996, **6**, 511.
9 K. J. Shea and D. A. Loy, *Mater. Res. Bull*., 2001, **5**, 358.
10 B. Boury and R. J. P. Corriu, *Chem. Commun*., 2002, 795.
11 B. Boury, and R. J. P. Corriu, in *The Chemistry of Organosilicon Compounds*, ed. Z. Rappoport and Y. Apeloig, John Wiley & Sons Ltd., Chichester, 2001, ch. 10, pp. 565.
12 *Functional Hybrid Materials*, ed. P. Gomez-Romero and C. Sanchez, Wiley-VCH, Weinheim, 2004.

13 C. Sanchez, B. Julian, P. Belleville and M. Popall, *J. Mater. Chem.*, 2005, **15**, 3559.
14 K. J. Shea, D. A. Loy and O. Webster, *J. Am. Chem. Soc.*, 1992, **114**, 6700.
15 K. M. Choi and K. J. Shea, *J. Phys. Chem.*, 1994, **98**, 3207.
16 K. M. Choi, J. C. Hemminger and K. J. Shea, *J. Phys. Chem.*, 1995, **99**, 4720.
17 H. W. Oviatt Jr, K. J. Shea, S. Kalluri, Y. Shi, W. H. Steier and L. R. Dalton, *Chem. Mater.*, 1995, **7**, 493.
18 D. A. Loy, G. M. Jamison, B. M. Baugher, S. A. Myers, R. A. Assink and K. J. Shea, *Chem. Mater.*, 1996, **8**, 656.
19 R. J. P. Corriu, J. J. E. Moreau, P. Thepot and M. Wong Chi Man, *Chem. Mater.*, 1996, **8**, 100.
20 R. J. P. Corriu, J. J. E. Moreau, P. Thepot and M. Wong Chi Man, *Chem. Mater.*, 1992, **4**, 1217.
21 S. W. Carr, M. Motevalli, D. L. Ou and A. C. Sullivan, *J. Mater. Chem.*, 1997, **7**, 865.
22 P. Chicart, R. J. P. Corriu, J. J. E. Moreau, F. Garnier and A. Yassar, *Chem. Mater.*, 1991, **3**, 8.
23 G. Cerveau, R. J. P. Corriu and C. Lepeytre, *J. Mater. Chem.*, 1995, **5**, 793.
24 R. J. P. Corriu, J. J. E. Moreau, P. Thepot, M. Wong Chi Man, C. Chorro, J.-P. Lere-Porte and J.-L. Sauvajol, *Chem. Mater.*, 1994, **6**, 640.
25 H. W. Oviatt Jr, K. J. Shea and J. H. Small, *Chem. Mater.*, 1993, **5**, 943.
26 C. Chuit, R. J. P. Corriu, G. Dubois and C. Reye, *Chem. Commun.*, 1999, 723.
27 G. Cerveau, R. J. P. Corriu and C. Lepeytre, *Chem. Mater.*, 1997, **9**, 2561.
28 J.-P. Bezombes, C. Chuit, R. J. P. Corriu and C. Reye, *J. Mater. Chem.*, 1998, **8**, 1749.
29 G. Cerveau, R. J. P. Corriu and N. Costa, *J. Non-Cryst. Solids*, 1993, **163**, 226.
30 P. Audebert, P. Calas, G. Cerveau, R. J. P. Corriu and N. Costa, *J. Electroanal. Chem.*, 1994, **372**, 275.
31 R. J. P. Corriu, P. Hesemann and G. F. Lanneau, *Chem. Commun.*, 1996, 1845.
32 D. C. Bookbinder and M. S. Wrighton, *J. Am. Chem. Soc.*, 1980, **102**, 5123.
33 J. G. Gaudiello, P. K. Ghosh and A. J. Bard, *J. Am. Chem. Soc.*, 1985, **107**, 3027.
34 P. Battioni, E. Cardin, M. Louloudi, B. Schollhorn, G. A. Spyroulias, D. Mansuy and T. G. Traylor, *Chem. Commun.*, 1996, 2037.
35 B. Lebeau, S. Brasselet, J. Zyss and C. Sanchez, *Chem. Mater.*, 1997, **9**, 1012.
36 B. Lebeau, C. Sanchez, S. Brasselet, J. Zyss, G. Froc and M. Dumont, *New J. Chem.*, 1996, **20**, 13.
37 B. Lebeau, J. Maquet, C. Sanchez, E. Toussaere, R. Hierle and J. Zyss, *J. Mater. Chem.*, 1994, **4**, 1855.
38 G. Dubois, R. J. P. Corriu, C. Reye, S. Brandès, F. Denat and R. Guilard, *Chem. Commun.*, 1999, **1**, 2283.
39 G. Dubois, C. Reye, R. J. P. Corriu and C. Chuit, *J. Mater. Chem.*, 2000, **10**, 1091.
40 S. T. Hobson and K. J. Shea, *Chem. Mater.*, 1997, **9**, 616.
41 E. Lindner, T. Schneller, F. Auer and H. A. Mayer, *Angew. Chem., Int. Ed.*, 1999, **38**, 2155.
42 F. Embert, A. Mehdi, C. Reye and R. J. P. Corriu, *Chem. Mater.*, 2001, **13**, 4542.
43 R. J. P. Corriu, E. Lancelle-Beltran, A. Mehdi, C. Reye, S. Brandès and R. Guilard, *Chem. Mater.*, 2003, **15**, 3152.
44 J. Livage and C. Sanchez, *J. Non-Cryst. Solids*, 1992, **145**, 11.
45 M. Henry and J. P. Jolivet, *Ultrastruct. Process. Adv. Mater., Proc. Int. Conf. Ultrastruct. Process. Ceram., Glasses Compos. 4th*, 1992, **4**, 20.
46 J. J. E. Moreau, L. Vellutini, M. Wong Chi Man, C. Bied, J.-L. Bantignies, P. Dieudonne and J.-L. Sauvajol, *J. Am. Chem. Soc.*, 2001, **123**, 7957.
47 J. J. E. Moreau, L. Vellutini, M. Wong Chi Man and C. Bied, *J. Am. Chem. Soc.*, 2001, **123**, 1509.
48 J. J. E. Moreau, L. Vellutini, M. Wong Chi Man and C. Bied, *Chem.–Eur. J.*, 2003, **9**, 1594.
49 C. Bied, J. J. E. Moreau, L. Vellutini and M. Wong Chi Man, *J. Sol–Gel Sci. Technol.*, 2003, **26**, 583.
50 J. J. E. Moreau, B. P. Pichon, M. Wong Chi Man, C. Bied, H. Pritzkow, J.-L. Bantignies, P. Dieudonne and J.-L. Sauvajol, *Angew. Chem., Int. Ed.*, 2004, **43**, 203.
51 J. J. E. Moreau, B. P. Pichon, C. Bied and M. Wong Chi Man, *J. Mater. Chem.*, 2005, **15**, 3929.
52 J. J. E. Moreau, L. Vellutini, P. Dieudonne, M. Wong Chi Man, J.-L. Bantignies, J.-L. Sauvajol and C. Bied, *J. Mater. Chem.*, 2005, **15**, 4943.
53 G. Cerveau, R. J. P. Corriu, F. Lerouge, N. Bellec, D. Lorcy and M. Nobili, *Chem. Commun.*, 2004, 396.
54 N. Bellec, F. Lerouge, B. Pichon, G. Cerveau, R. J. P. Corriu and D. Lorcy, *Eur. J. Org. Chem.*, 2005, 136.
55 (*a*) G. Cerveau, R. J. P. Corriu and E. Framery, *Chem. Commun.*, 1999, 2081; (*b*) G. Cerveau, R. J. P. Corriu and E. Framery, *J. Mater. Chem.*, 2000, **10**, 1617; (*c*) G. Cerveau, R. J. P. Corriu and E. Framery, *J. Mater. Chem.*, 2001, **11**, 713; (*d*) G. Cerveau, R. J. P. Corriu, E. Framery, S. Ghosh and H. Mutin, *J. Mater. Chem.*, 2002, **12**, 3021.
56 (*a*) G. Cerveau, R. J. P. Corriu and C. Fischmeister-Lepeytre, *J. Mater. Chem.*, 1999, **9**, 1149; (*b*) G. Cerveau, R. J. P. Corriu and E. Framery, *Polyhedron*, 2000, **19**, 307; (*c*) G. Cerveau, R. J. P. Corriu and E. Framery, *C. R. Acad. Sci., Ser. IIc: Chim.*, 2001, **4**, 79.
57 G. Cerveau, R. J. P. Corriu and E. Framery, *Chem. Mater.*, 2001, **13**, 3373.
58 A. N. Parikh, M. A. Schivley, E. Koo, K. Seshadri, D. Aurentz, K. Mueller and D. L. Allara, *J. Am. Chem. Soc.*, 1997, **119**, 3135.
59 A. Shimojima and K. Kuroda, *Langmuir*, 2002, **18**, 1144.
60 (*a*) A. Shimojima, D. Mochizuki and K. Kuroda, *Chem. Mater.*, 2001, **13**, 3603; (*b*) A. Shimojima, N. Umeda and K. Kuroda, *Chem. Mater.*, 2001, **13**, 3610.
61 A. Shimojima and K. Kuroda, *Chem. Lett.*, 2000, 1310.
62 A. Shimojima, Y. Sugahara and K. Kuroda, *J. Am. Chem. Soc.*, 1998, **120**, 4528.
63 H. L. Cabibil, V. Pham, J. Lozano, H. Celio, R. M. Winter and J. M. White, *Langmuir*, 2000, **16**, 10471.
64 L. Ukrainczyk, R. A. Bellman and A. B. Anderson, *J. Phys. Chem. B*, 1997, **101**, 531.
65 C. R. Silva, M. G. Fonseca, J. S. Barone and C. Airoldi, *Chem. Mater.*, 2002, **14**, 175.
66 M. Jaber, J. Miehe-Brendle and R. Le Dred, *Chem. Lett.*, 2002, 954.
67 M. G. da Fonseca and C. Airoldi, *J. Mater. Chem.*, 2000, **10**, 1457.
68 M. G. da Fonseca, C. R. Silva, J. S. Barone and C. Airoldi, *J. Mater. Chem.*, 2000, **10**, 789.
69 J. Alauzun, A. Mehdi, C. Reye and R. J. P. Corriu, *J. Am. Chem. Soc.*, 2005, **127**, 11204.
70 (*a*) R. J. P. Corriu, J. J. E. Moreau, P. Thepot, M. Wong Chi Man, C. Chorro, J.-P. Lere-Porte and J.-L. Sauvajol, *Chem. Mater.*, 1994, **6**, 640; (*b*) R. J. P. Corriu, J. J. E. Moreau, P. Thepot, C. Chorro, J.-P. Lere-Porte, J.-L. Sauvajol and M. Wong Chi Man, *Synth. Met.*, 1994, **62**, 233.
71 R. J. P. Corriu, J. J. E. Moreau, P. Thepot and M. Wong Chi Man, *Chem. Mater.*, 1996, **8**, 100.
72 (*a*) R. J. P. Corriu, F. Imbert, Y. Guari, C. Reye and R. Guilard, *Chem.–Eur. J.*, 2002, **8**, 5732; (*b*) R. J. P. Corriu, A. Mehdi, C. Reye and C. Thieuleux, *New J. Chem.*, 2003, **27**, 905.
73 (*a*) G. Dubois, C. Reye, R. J. P. Corriu, S. Brandes, F. Denat and R. Guilard, *Angew. Chem., Int. Ed.*, 2001, **40**, 1087; (*b*) J. Goulon, C. Goulon-Ginet, A. Rogalev, F. Wilhelm, N. Jaouen, D. Cabaret, Y. Joly, G. Dubois, R. J. P. Corriu, G. David, S. Brandès and R. Guilard, *Eur. J. Inorg. Chem.*, 2005, **13**, 2714.
74 (*a*) B. Boury, R. J. P. Corriu, P. Delord, M. Nobili and V. Le Strat, *Angew. Chem., Int. Ed.*, 1999, 3172; (*b*) F. Ben, B. Boury, R. J. P. Corriu and V. Le Strat, *Chem. Mater.*, 2000, **12**, 3249; (*c*) B. Boury, F. Ben, R. J. P. Corriu, M. Nobili and P. Delord, *Chem. Mater.*, 2002, **14**, 730.

75 A. Vergnes, M. Nobili, P. Delord, L. Cipelletti, R. J. P. Corriu and B. Boury, *J. Sol–Gel Sci. Technol*., 2003, **26**, 621.
76 (*a*) B. Boury, F. Ben and R. J. P. Corriu, *Adv. Mater*., 2002, **14**, 101; (*b*) G. Cerveau, R. J. P. Corriu, E. Framery and F. Lerouge, *Chem. Mater*., 2004, **16**, 3794; (*c*) G. Cerveau, R. J. P. Corriu, E. Framery and F. Lerouge, *J. Mater. Chem*., 2004, **14**, 3019; (*d*) F. Lerouge, G. Cerveau and R. J. P. Corriu, unpublished results.
77 F. Lerouge, G. Cerveau and R. J. P. Corriu, *J. Mater. Chem*., 2006, **16**, 90.
78 A. Pegenau, T. Hegmann, C. Tschierske and S. Diele, *Chem.–Eur. J*., 1999, **5**, 1643.
79 H. Helker and R. Hatz, *Handbook of Liquid Crystals*, Verlag Chemie, Weinheim, Germany, 1980.
80 P. Grosshanns, A. Jouaiti, V. Bulach, J.-M. Planeix, M. W. Hosseini and J.-F. Nicoud, *Chem. Commun*., 2003, 1336.

